

PACS numbers: 68.37.Hk, 75.50.Bb, 75.75.Cd, 81.07.Wx, 81.20.Ev, 81.20.Wk, 81.40.Rs

Structural, Morphological, and Magnetic Properties of the Binary $\text{Fe}_{60}\text{Co}_{40}$ Alloy Synthesized by Mechanical Alloying Processing

Ahmed Y. Khidhaeir¹, I. K. Jassim², and Raed H. AL-Saqa¹

¹*College Education of Pure Science,
Department of Physics,
Tikrit University,
Tikrit, Iraq*

²*College of Medical Techniques,
AL-Kitab University,
AL-Kitab, Iraq*

Nanocrystalline of $\text{Fe}_{60}\text{Co}_{40}$ powders are prepared by mechanical alloying using ball milling technique (BMT) under several milling times (of 0, 1, 3, 5 hrs). Structural diffractometry (XRD), scanning electron microscopy (SEM), element dispersive spectroscopy (EDS), and the vibrating sample magnetometry (VSM) are used for investigation of the structural changes, magnetic and morphological properties during the milling times. XRD analysis suggests the face-centred cubic (f.c.c.) phase formed successfully after initial milling time. The particle sizes are decreased significantly with the milling time. The SEM results show that particles of all practical sizes are approximately of spherical shapes with uniform sizes. The EDS results show no strange elements in the milling media. The magnetic properties appear to be sensitive to milling times. The saturation magnetization (M_s) is found to increase with increasing milling time, but the coercivity (H_c) is found to decrease, so that the $\text{Fe}_{60}\text{Co}_{40}$ -nanoalloy powder exhibits a soft ferromagnetic character.

Нанокристалічні порошки $\text{Fe}_{60}\text{Co}_{40}$ було одержано шляхом механічного стоплення за допомогою техніки кульового млину за кілька часів розмелювання (0, 1, 3, 5 годин). Використано рентгенівську дифрактометрію (XRD), сканувальну електронну мікроскопію (SEM), елементну дисперсійну спектроскопію (EDS) та вібраційну магнетометрію (VSM) для ретельного дослідження структурних змін, морфологічних і магнетних властивостей під час розмелювання. XRD-аналіза показала, що гранецентрована кубічна (ГЦК) фаза успішно утворилася після початкового часу розмелювання. Розмір частинок значно зменшувався з часом розмелювання. Результати SEM показали, що частинки усіх практичних розмірів є приблизно сферичної форми з однаковими розмірами. Ре-

зультати EDS не показали дивних елементів у розмелювальному середовищі. Магнетні властивості виявилися чутливими до часу розмелювання. Було виявлено, що намагнетованість насити (M_s) збільшується зі збільшенням часу розмелювання, але коерцитивність (H_c) зменшується, так що порошок наностопу $\text{Fe}_{60}\text{Co}_{40}$ демонструє м'який феромагнетний характер.

Key words: $\text{Fe}_{60}\text{Co}_{40}$ nanoalloy, nanostructures, saturation magnetization, coercivity.

Ключові слова: наностоп $\text{Fe}_{60}\text{Co}_{40}$, наноструктури, намагнетованість насити, коерцитивність.

(Received 25 November, 2023)

1. INTRODUCTION

Nanoalloys present an intriguing theoretical problem, in fact, the presence of two distinct atom types increases the complexity of bimetallic nanoalloys, opening the door to the possibility of isomers based on the permutation of unlike atoms as well as regular geometrical isomers (with different skeletal structures), (A_mB_n) alloy cluster structures with a fixed number of atoms ($N = m + n$) and composition (m/n ratio) are referred to as 'homotopic' because they have the same geometrical arrangement of atoms but differ in the arrangement of A- and B-type atoms [1].

Because of their many uses in magnetic separation, microwave absorbers, magnetic fluids, magnetic sensors, and magnetic recording systems, magnetic nanomaterial are a subject of growing research [2, 3].

There is a wide range of literature studies of magnetic transition elements and alloys such as nickel (Ni), cobalt (Co), iron (Fe), or composites [4, 5]. These nanomaterials have become the subject of large-scale research due to their high saturation magnetization (M_s), relatively low coercive field (H_c), and fairly large Curie temperature (T_c) [6].

Several specific techniques and development approaches have been adopted to synthesize nanostructured Fe–Ni, Ni–Co, and Fe–Ni–Cr alloys [7].

One of the most widely used methods for preparation is mechanical alloying (MA), as well as the powder technique (PT) method [8]. During the MA process, the powder particles are subjected to severe mechanical deformation, leading to their gradual refinement at the nanoscale [9]. Therefore, we investigate the structural, magnetic, and morphological powder properties of the $\text{Fe}_{60}\text{Co}_{40}$ nanoalloy prepared by the mechanical alloying process after 0, 1, 3, and 5 hrs

milling times.

2. EXPERIMENTAL PROCEDURES

Commercial Fe and Co powders with particle sizes of 40 μm were milled using a planetary ball miller. Pluck initial elemental iron and nickel of highly 99.93% purity have been used as starting materials with particle sizes around 40 μm for both elements, and they were mixed at the desired composition of the $\text{Fe}_{60}\text{Co}_{40}$ alloy.

The milling practical was conducted using 40 hardened balls with a diameter of 10 mm at room temperature. The weight ratio of the ball to powder was set at 40:1 grams. We employed the variable milling times of 0, 1, 3, and 5 hours. 135 rpm was the rotation speed. Energy dispersive spectrometry (EDS) equipped scanning electron microscopy (SEM) with Model Philips (XL30) was used to assess morphology and conduct elemental analysis. The powdered powders' precisely defined structure and phase changes were observed. The magnetization properties are derived from the hysteresis loops by using a vibrating sample magnetometry (VSM) device. Finally, the structure was characterized by x-ray diffraction (XRD) using a Philips (PW 1820) diffractometer equipped with a CuK_α radiation source (wave length = 1542 \AA).

3. RESULTS AND DISCUSSION

Figure 1 shows the XRD patterns of the $\text{Fe}_{60}\text{Co}_{40}$ nanoalloy with varying milling times (0, 3, and 5 hrs). As revealed from XRD pat-

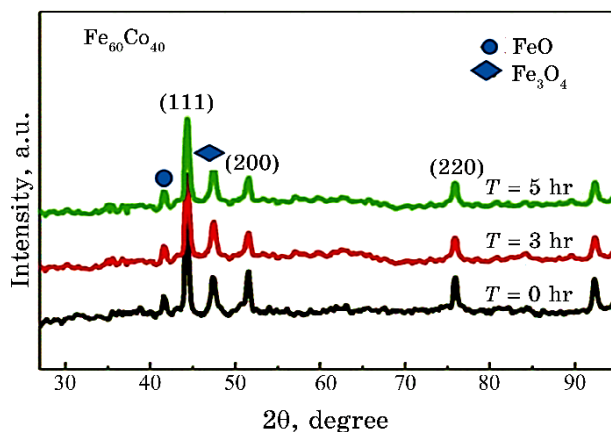


Fig. 1. XRD patterns of the $\text{Fe}_{60}\text{Co}_{40}$ alloy with various milling times (0, 3, 5 hours).

terns, the peaks at 44.32° , 51.80° , and 76.20° correspond to the crystal planes of (111), (200), and (220), respectively, of face-centred cubic (f.c.c.) lattice, which are in closer agreement with the reported articles [10, 11]. In addition, the diffraction peaks of 41.5° and 47.5° may represent FeO and Fe_3O_4 , respectively [12]. This may be due to the exposure of heat through the mechanical alloying that generated the oxide layers [11]. No diffraction peaks related to the h.c.p. phase are detected for cobalt (Co) at milling times. The other result shows that, by using the Scherrer equation for the calculation of particle size, we found all values to be close to 19.30 nm for all samples at various milling times [12].

These results mean that the size of the nanocrystalline $\text{Fe}_{60}\text{Co}_{40}$ is nondependent on the $\text{Fe}_{60}\text{Co}_{40}$ -nanoalloy composition through the milling time [13].

The magnetic properties results of the $\text{Fe}_{60}\text{Co}_{40}$ nanoalloy were measured using VSM at room temperature (RT) to determine the values of saturation magnetization (M_s) and coercivity (H_c), as shown in Fig. 2. It shows the M - H curves at various milling times of 1, 3, and 5 hrs measured in an external magnetic field, ranging from -10 to 10 kOe. The results show that the saturation magnetization (M_s) increases with the increase in milling time, but the coercivity (H_c) decreases with the increase in milling time. Their maximum (M_s) and minimum (H_c) were found to be close to 104.88 emu/gm and 56.95 Oe for the $\text{Fe}_{60}\text{Co}_{40}$ nanoalloy, respectively (Fig. 3). The present results show a clearer agreement than those reported in the literature [13, 14].

Finally, the results obtained from the magnetic properties of the $\text{Fe}_{60}\text{Co}_{40}$ nanoalloy can indicate that the sample has soft magnetic behaviour and can be used for various practical applications [15].

The SEM-images' results for the $\text{Fe}_{60}\text{Co}_{40}$ nanoalloy are presented in Fig. 4, *a-d* for 1, 3, and 5 hours milling times. It shows clearly in Fig. 4, *a*, after 1 hour of milling, the particles were no longer uniform and began to combine. After 3 hours of milling, a changeable structure was observed, indicating that the two elements are probably alloyed completely and formed [16]. All particle sizes in Fig. 4, *b, c* are approximately spherical in shape and uniform in size. The composite ($\text{Fe}_{60}\text{Co}_{40}$) particles are formed completely (Fig. 4, *b, c*) with a spherical shape morphology and aggregated themselves into a cluster of particles. The agglomeration is probably due to the high cold-welding rate that occurs during the milling process [17].

Latterly, as seen in Fig. 5, elemental mapping by (EDS) coupled to the (SEM) displays the spectroscopy of Fe and Co distribution for the sample areas, which were chosen at the 5-h milling period. It is made abundantly evident that iron and cobalt are still easily distin-

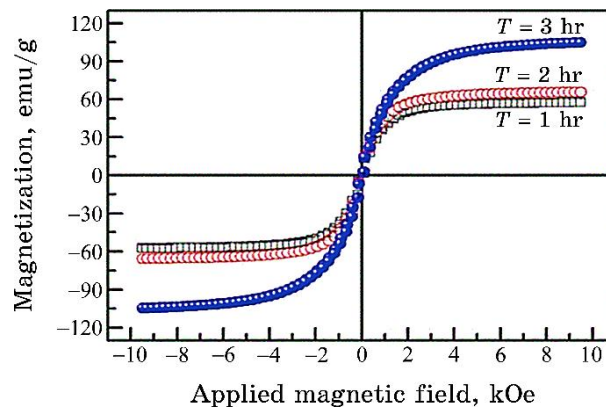


Fig. 2. The magnetic properties at various milling times (1, 2, 3 hours).

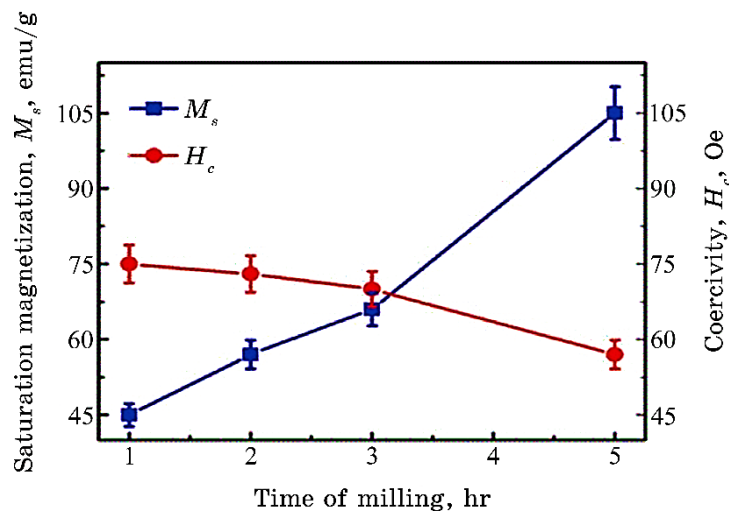


Fig. 3. The magnetic properties of $\text{Fe}_{60}\text{Co}_{40}$ nanoalloy at various milling times.

guished from one another. This means that Fe and Co are a completely alloying processed. These EDS results actually match and are consistent with the XRD study. They both observed that there was no elemental contamination.

4. CONCLUSION

XRD, SEM, EDS, and VSM experiments were used to examine the impact of mechanical alloying on the structural, morphological, and

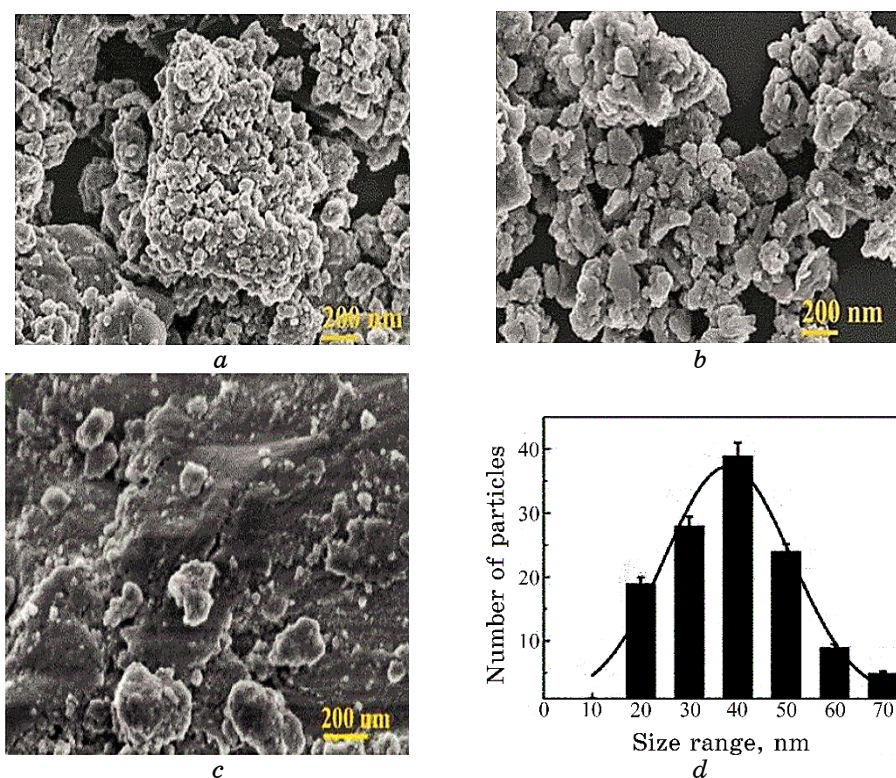


Fig. 4. SEM images for Fe₆₀Co₄₀ nanoalloy at various milling times: *a*—1 hr, *b*—3 hr, *c*—5 hr; *d*—particle size distribution.

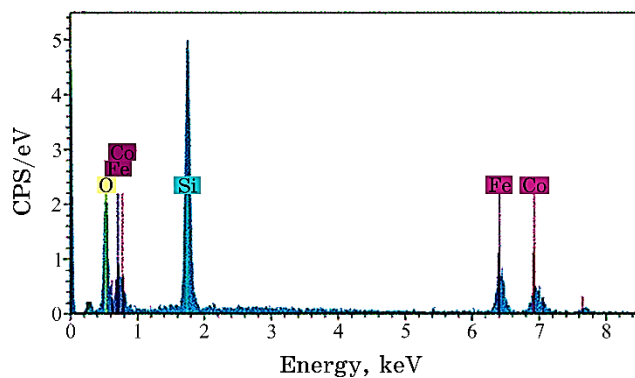


Fig. 5. EDS spectra for Fe₆₀Co₄₀ nanoalloy at 5-hours milling time.

magnetic properties of the Fe₆₀Co₄₀ nanoalloy, which was created from pure elemental Co and Fe powders.

XRD analysis indicates the formation of a main face-centred cubic (f.c.c.) structure of Fe–Co solid phase.

SEM micrographs reveal spherical-shaped particles and a homogeneous size distribution.

EDS results show no strange element during milling times.

The magnetic properties of the Fe₆₀Co₄₀ nanoalloy powder show that they are sensitive to milling times and exhibit soft ferromagnetic behaviour.

ACKNOWLEDGMENT

First and foremost, we would like to express our gratitude to the faculty and staff of the Universities of Tikrit (Iraq) and Al-Kitab (Iraq) for their significant contributions, insightful conversations, and ongoing support during our quest.

REFERENCES

1. R. Ferrando, J. Jellinek, and R. L. Johnston, *Chemical Reviews*, **108**, No. 3: 845 (2008); doi:10.1021/cr040090g
2. Hosam M. Saleh and Amal I. Hassan, *Sustainability*, **15**, No. 14: 10891 (2023); <https://doi.org/10.3390/su151410891>
3. M. L. Silva, M. A. Morales, J. F. M. L. Mariano, J. A.H. Coaquira, and J. H. de Araújo, *Journal of Alloys and Compounds*, **963**, No. 10: 171285 (2023); <https://doi.org/10.1016/j.jallcom.2023.171285>
4. L. A. Frolova and T. Ye. Butyrina, *Nanosistemi, Nanomateriali, Nanotehnologii*, **19**, Iss. 2: 0263 (2021); <https://doi.org/10.15407/nnn.19.02.263>
5. O. M. Berdnikova, Yu. M. Tyurin, O. V. Kolisnichenko, O. S. Kushnarova, Ye. V. Polovetskiy, E. P. Titkov, and L. T. Yermeyeva, *Nanosistemi, Nanomateriali, Nanotehnologii*, **20**, Iss. 1: 97 (2022); <https://doi.org/10.15407/nnn.20.01.097>
6. L. Aymard, B. Dumont, and G. Viau, *Journal of Alloys and Compounds*, **242**, Nos. 1–2: 108 (1996); [https://doi.org/10.1016/0925-8388\(96\)02285-2](https://doi.org/10.1016/0925-8388(96)02285-2)
7. I. K. Jassim, K.-U. Neumann, D. Visser, P. J. Webster, and K. R. A. Ziebeck, *Physica B: Condensed Matter*, **180–181**, No. 1: 145 (1992); [https://doi.org/10.1016/0921-4526\(92\)90688-O](https://doi.org/10.1016/0921-4526(92)90688-O)
8. A. Mukhtar, T. Mehmood, and K. M. Wu, *IOP Conference Series Materials Science and Engineering (Online)*, **239**, No. 1: 5 (2017); doi:10.1088/1757-899X/239/1/012017
9. B. Neelima, N. V. Rama Rao, V. Rangadhara Chary, and S. Pandian, *Journal of Alloys and Compounds*, **661**, No. 72: 76 (2016); <https://doi.org/10.1016/j.jallcom.2015.11.186>
10. Ahmed Y. Khidhaeir and Ismail K. Jassim, *International Journal of Scientific Research in Science and Technology (IJSRST)*, **10**, No. 5: 391 (2023); <https://doi.org/10.32628/IJSRST52310528>
11. H. Shokrollahi, *Materials & Design*, **30**, No. 9: 3374 (2009); <https://doi.org/10.1016/j.matdes.2009.03.035>

12. A. Ayuela, J. Enkovaara, K. Ullakko, and R. Nieminen, *Journal of Physics: Condensed Matter*, **11**: 2017 (1999); doi [10.1088/0953-8984/11/8/014](https://doi.org/10.1088/0953-8984/11/8/014)
13. K. Ibrahim, S. Khalid, and K. Idrees, *Arabian Journal of Chemistry*, **12**, No. 7: 908 (2019); <https://doi.org/10.1016/j.arabjc.2017.05.011>
14. E. Michael, D. McHenry, and E. Laughlin, *Physical Metallurgy*, **1881**: 2008 (2014); <https://doi.org/10.1016/B978-0-444-53770-6.00019-8>
15. M. Mhadhbi and W. Polkowski, *Crystals*, **12**: 1280 (2022); <https://doi.org/10.3390/cryst12091280>
16. A. F. Al-Falahi and A. Hameed, *Al-Kitab Journal for Pure Sciences*, **3**, No. 1: 15 (2023); <https://doi.org/10.32441/kjps.03.01>
17. R. Raimundo, V. Silva, L. Ferreira, F. Loureiro, D. Fagg, D. Macedo, U. Gomes, M. Soares, R. Gomes, and M. Morales, *Magnetochemistry*, **9**, No. 8: 201 (2023); <https://doi.org/10.3390/magnetochemistry9080201>